Published as: *Nat Neurosci*. ; 15(3): 449–S2.

Activity Recall in Visual Cortical Ensemble

Shengjin Xu[1,2,*], **Wanchen Jiang**[1,2,*], **Mu-ming Poo**[1,3,+], and **Yang Dan**[3,4]

[1]Institute of Neuroscience, State Key Laboratory of Neuroscience, Shanghai Institutes for Biological Sciences, Chinese Academy of Sciences, Shanghai, China 200031

[2]Graduate School of the Chinese Academy of Sciences, Shanghai, China 200031

[3]Division of Neurobiology, Department of Molecular and Cell Biology, Helen Wills Institute of Neuroscience, University of California, Berkeley, CA 94720, U.S.A.

[4]Howard Hughes Medical Institute, University of California, Berkeley, CA 94720, U.S.A.

Abstract

Cue-triggered recall of learned temporal sequences is an important cognitive function that has been attributed to higher brain areas. Here, recordings in both anesthetized and awake rats demonstrate that after repeated stimulation with a moving spot that evoked sequential firing of an ensemble of primary visual cortex (V1) neurons, just a brief flash at the starting point of the motion path was sufficient to evoke a sequential firing pattern that reproduced the activation order evoked by the moving spot. The speed of recalled spike sequences may reflect the internal dynamics of the network rather than the motion speed. In awake animals, such recall was observed during a synchronized ("quiet wakeful") brain state with large-amplitude, low-frequency local field potential (LFP), but not in a desynchronized ("active") state with low-amplitude, high-frequency LFP. Such conditioning-enhanced, cue-evoked sequential spiking of a V1 ensemble may contribute to experience-based perceptual inference in a brain state-dependent manner.

An essential feature of memory recall is pattern completion, in which the retrieval of memory is triggered by a subset of the cues present during learning. In particular, cue-triggered recall of a learned temporal sequence is useful for predicting future events based on current sensory inputs[1, 2]. Studies of episodic memory in human subjects have strongly indicated the role of the hippocampus and its surrounding cortical areas in the learning and recall of temporal sequences[3, 4]. Experiments in the rat also showed that hippocampal lesions can cause selective impairments of the ability to remember the temporal sequence of recently experienced sensory stimuli or spatial locations[5-7]. Furthermore, simultaneous recordings from a large number of hippocampal neurons have revealed spontaneous

[+]To whom the correspondence should be addressed. mpoo@berkeley.edu.
[*]These authors contributed equally to this work

AUTHOR CONTRIBUTIONS

S. X. and W. J. conducted all experiments and performed all data analyses; S. X., W. J., M.-m. P., and Y.D. designed the experiments and wrote the manuscript.

Competing financial interests

The authors declare no competing financial interests.

reactivation of the spike sequences observed during active exploration in subsequent periods of sleep or awake immobility[8-13]. These findings have pointed to the experience-dependent enhancement of sequential spiking in the hippocampus as a potential neural mechanism for sequence learning and memory. However, whether learning of simple sequences can also occur in early sensory circuits remains unclear.

Experience-dependent modifications in early sensory circuits are believed to contribute to some forms of perceptual learning. In the somatosensory[14] and auditory[15] cortex, learning causes an increased cortical representation of the learned stimuli. In the human visual system, the location, orientation, or spatial frequency specificity of training-induced improvement in pattern discrimination suggests an involvement of early visual circuits[16, 17]. Functional MRI studies further showed that learning in visual detection is accompanied by an increase in V1 activity[18]. Electrophysiological studies in awake monkeys have shown that training in orientation discrimination causes a change in the tuning curves of V1 neurons[19], and learning in shape discrimination causes changes in the contextual modulation of V1 neuronal responses[20]. Although these studies provided ample evidence for learning-related modification in adult V1, change related to sequence learning has not been demonstrated.

In this study, we tested learning and recall of a simple motion sequence in V1. Since V1 neurons have well-defined receptive fields (RFs), we used a moving spot to evoke sequential firing of the ensemble of neurons whose RFs fall along the motion path. Shortly after repeated motion conditioning, a briefly flashed spot at the starting point of the motion path evoked more sequential spiking similar to that evoked by the moving spot, reminiscent of cue-triggered recall of a learned temporal sequence. This recall effect was specific to the trajectory of the repeated motion, and in awake animals it depended on the brain state. Thus, cue-triggered recall of a simple spike sequence can occur in an early sensory circuit and may contribute to experience-based perceptual inference.

RESULTS

A multielectrode array with 2 × 8 channels was used to record the spiking activity of a neuronal ensemble in V1 of either urethane-anesthetized (Supplementary Fig. 1a) or awake head-fixed rat (Fig. 1a and Supplementary Movie 1; see Online Methods). The multiunit RFs mapped with sparse noise stimuli were distributed in a ~100 × 25 region of the visual field (Fig. 1b, c and Supplementary Fig. 1b, c), in a manner consistent with the retinotopic map of rat V1. Although eye movement was observed in the awake head-fixed animals, the amplitudes were much smaller than the average RF size (s.d. < 10% RF size, Supplementary Fig. 2), consistent with previous studies[21, 22]. Accordingly, the RFs in the awake rats were highly stable over time (Fig. 1b) and similar in size to those measured in anesthetized animals (Supplementary Fig. 1b, c), whose eyes were stabilized mechanically (see Online Methods). To evoke sequential spiking of the recorded neurons, we presented a conditioning stimulus consisting of a bright spot (anesthetized: 13.5°; awake: 18° in diameter) moving repeatedly from *S* (starting point) to *E* (end point), across the long axis of the RF distribution (speed 180° s^{-1}, repeated once every 2.1 – 2.3 s, 100 trials; Fig. 1c and Supplementary Fig. 1c). In both anesthetized and awake rats, this conditioning stimulus evoked strong spiking

responses with the firing sequence largely consistent with the RF locations along the motion trajectory (Fig. 1d and Supplementary Fig. 1d). The Spearman (rank-order) correlation coefficients (CCs) between the firing time of the recorded units and their RF locations along the $S \rightarrow E$ axis were 0.94 ± 0.08 (awake, mean ± s.d., n = 18 experiments) and 0.91 ± 0.09 (anesthetized, n = 19 experiments).

Conditioning-induced increase in sequential spiking

To assess learning of this motion sequence by the cortical ensemble, we briefly presented the bright spot at the starting point of the motion path (*S*) as the test cue and examined the spike sequence within the cortical ensemble. Figure 2a, b shows the spike trains of simultaneously recorded multiunits evoked by the test cue at *S* in several consecutive trials before (top row) and after (bottom row) 100 repeats of the motion conditioning (middle row), with the units ordered by their RF locations along the $S \rightarrow E$ axis. The test cue-evoked spike trains in Figure 2b are shown at an expanded time scale, since the recall in awake animals was found to occur at a faster speed (see below). Prior to the conditioning, the responses in some test trials exhibited sequential spiking, but the firing sequence was quite variable across trials. In the trials after conditioning, we found a marked increase in sequential spiking similar to that evoked by the conditioning motion stimuli.

To further demonstrate such sequential spiking, we adopted a pairwise correlation analysis previously used to characterize spontaneous sequence replay in the hippocampus and prefrontal cortex[11, 23]. Briefly, we computed the cross-correlation between each pair of spike trains for all pairwise combinations of simultaneously recorded units in each experiment; the correlation was then plotted against both the temporal delay between the pair and their RF distance. For the responses to conditioning motion, the peak of correlation showed a prominent rightward shift with the RF distance in both anesthetized and awake animals (upper row; Fig. 2c, d). This lower left to upper right slant of the correlation function represents an increase in the relative spike timing of the pair with their RF distance, thus serving as a reliable indicator for sequential spiking within the ensemble. For the responses evoked by the test cue at *S*, there was a slight slant of the correlation function before conditioning (second row; Fig. 2c, d). This is because the response to a flashed stimulus generally exhibits some horizontal spread within the cortex[24]. Although the response to the test cue at *S* is expected to spread symmetrically from *S* (both towards and away from *E*), the recorded neurons were all on one side of *S* (towards *E*). The slight slant in the correlation function among these units thus reflects the spread of the response. Notably, there was a marked increase in the slant after conditioning (third row; Fig. 2c, d). The conditioning-induced change is also shown by the difference function ("*After – Before*", bottom row), which revealed an increase in correlation at positive timing and a decrease at negative timing with a similar slant. This indicates that the motion conditioning enhanced test cue-evoked sequential spiking of the cortical ensemble in the $S \rightarrow E$ direction. This effect was not accompanied by any significant change in the mean firing rates of the neurons (anesthetized, $P = 0.80$, n = 18 experiments; awake, $P = 0.84$, n = 19; Wilcoxon signed rank test), indicating that the effect was due to changes in the relative timing rather than the rate of neuronal spiking. Such a conditioning-induced modification of the cue-evoked ensemble

spike pattern provides a potential neural mechanism for learning and recall of the motion sequence.

Specificity of sequence recall

To analyze the effect of conditioning on sequential spiking quantitatively, we computed for each test trial the Spearman CC between the firing time of the units and their RF locations along the $S \rightarrow E$ axis (see Online Methods). As shown in the cumulative histograms of CCs (Fig. 3a, b), 100 trials of motion conditioning at a speed of 180° s^{-1} caused a significant rightward shift of the CC distribution in both anesthetized (mean CC from 0.21 to 0.29, $P = 1.5 \times 10^{-3}$, n = 19 experiments; Kolmogorov-Smirnov test) and awake (mean CC from 0.22 to 0.30, $P = 1.5 \times 10^{-4}$, n = 18) animals, indicating increased sequential firing along the $S \rightarrow E$ trajectory. Instead of correlation between the firing time and RF location, we also computed the Spearman CC between the neuronal firing time for *S*-evoked responses and that for conditioning stimulus-evoked responses. We found a similar rightward shift of the CC distribution after conditioning (Supplementary Fig. 3).

Note that the CC distribution for *S*-evoked responses showed a rightward bias even before conditioning (dotted line; Fig. 3a, b). As explained above, this reflects the symmetric spread of the activity evoked by the test cue at *S*. To eliminate this bias, we performed additional experiments in awake rats with the test spot flashed at the mid-point between *S* and *E* (see Online Methods). As expected, we found no rightward bias in the CC distribution before conditioning (dotted line; Fig. 3c), as the RFs of the recorded units were distributed on both sides of the test spot. Nevertheless, 100 trials of $S \rightarrow E$ conditioning still caused a significant rightward shift of the CC distribution (mean CC from −0.08 to −0.02, $P = 1.3 \times 10^{-4}$, n = 19 experiments; Kolmogorov-Smirnov test; solid line; Fig. 3c). Furthermore, to test whether the observed recall was specific to the conditioned motion sequence ($S \rightarrow E$), we analyzed the response to the test stimulus presented at the end point (*E*), which in principle could evoke an $E \rightarrow S$ spike sequence. Before conditioning, the CC between the timing of *E*-evoked spiking and the RF position along the $E \rightarrow S$ axis also showed a rightward bias (dotted line; Fig. 3d and Supplementary Fig. 4a) that was not significantly different from that for *S*-evoked spiking (dotted line; Fig. 3a, b; awake: $P = 0.58$, n = 18 experiments; anesthetized: $P = 0.26$, n = 19; Kolmogorov-Smirnov test), again reflecting the symmetric spread of cortical response. However, unlike for the *S*-evoked responses, we found no significant change in the CC distribution for the *E*-evoked spiking after $S \rightarrow E$ conditioning (awake: mean CC from 0.20 to 0.20, $P = 0.59$, n = 18 experiments; anesthetized: mean CC from 0.20 to 0.21, $P = 0.77$, n = 19; Kolmogorov-Smirnov test; Fig. 3d and Supplementary Fig. 4a). Thus, instead of a non-specific increase in the horizontal spread of the cortical response to a flashed stimulus, $S \rightarrow E$ conditioning caused a selective increase in sequential firing in the $S \rightarrow E$ direction. Furthermore, we found that 100 trials of conditioning along a motion path parallel to, but not overlapping with, the long axis of the recorded RF distribution (at a distance of 27° – 45°) caused no significant change in the CC distribution for either *S*- or *E*-evoked spiking (*S*: mean CC from 0.37 to 0.36, $P = 0.80$, n = 14; *E*: mean CC from 0.42 to 0.40, $P = 0.93$; Kolmogorov-Smirnov test; Supplementary Fig. 5), indicating that the effect was also specific to the position of the motion sequence rather than reflecting a general change in the direction of spike propagation in the visual cortex.

To further confirm the importance of the sequential excitation evoked by the $S \rightarrow E$ conditioning, we used a flashed bar spanning the region between *S* and *E* as the conditioning stimulus in awake rats (see Online Methods). We found that 100 trials of the bar conditioning caused no significant change in the CC distribution for the test cue at *S* (mean CC from 0.22 to 0.22, $P = 0.76$, n = 18 experiments; Kolmogorov-Smirnov test; Fig. 3e) or *E* (mean CC from 0.19 to 0.19, $P = 0.62$; Fig. 3f), although they caused a small but significant increase in the mean firing rates of the neurons (from 10.5 ± 0.1 to 11.0 ± 0.3, mean ± s.e.m., $P = 0.03$, Wilcoxon signed rank test). A previous study using voltage-sensitive dye imaging (VSDI) showed that following repeated flashes of a bright stimulus at a given retinal location, the spatiotemporal patterns of spontaneous cortical waves became more similar to the cortical response evoked by the flashed stimulus[25]. We thus tested whether such a flashed conditioning stimulus at *S* can cause an increase in sequential firing. As shown in Supplementary Figure 4b, c, 100 flashes of the bright spot caused no significant change in CC distribution for the test cue at *S* (mean CC from 0.30 to 0.31, $P = 0.47$, n = 17 experiments; Kolmogorov-Smirnov test) or *E* (mean CC from 0.32 to 0.32, $P = 0.44$). Together, these experiments indicate that the static conditioning stimuli are not sufficient to cause the increase in sequential firing.

In the experiments above, the electrode array was always implanted in V1 at an orientation similar to that illustrated in Figure 1a. To test whether the effect was specific to this cortical axis, we performed another set of experiments with the electrode array implanted at a new orientation (Supplementary Fig. 6a), with corresponding changes in the RF distribution (Supplementary Fig. 6b). We found that $S \rightarrow E$ conditioning also caused a marked increase in the slant of the pairwise cross-correlation function (Supplementary Fig. 6c) and a significant rightward shift of the CC distribution for the test cue at *S* (mean CC from 0.28 to 0.37, $P = 4.3 \times 10^{-5}$, n = 18 experiments; Kolmogorov-Smirnov test; Supplementary Fig. 6d), but not at *E* (mean CC from 0.31 to 0.29, $P = 0.53$; Supplementary Fig. 6e). Thus, the increase in sequential firing induced by the motion conditioning was not restricted to a particular cortical axis.

Further characterization of sequence recall

To facilitate further characterization of the effect of conditioning, we defined a ‘match’ as a test trial whose Spearman CC is above a given threshold and compared the percentage of matches before and after conditioning in each experiment. We found that the percentage increased significantly after conditioning over a wide range of CC thresholds for both awake and anesthetized animals for test cue at *S* (black line; Fig. 4a and Supplementary Fig. 7a), but not at *E* (gray line). To examine the persistence of the effect, we plotted the increase in the percentage of matches (at CC threshold of 0.6) measured at different times after 100 trials of conditioning. Within a period of ~7 min, the effect decayed completely for awake (Fig. 4b, c) and partially for anesthetized (Supplementary Fig. 7b, c) animals. We then tested whether the magnitude and persistence of the effect depend on the number of conditioning trials in anesthetized rats. As shown in Figure 5a, significant effect was found after 50, 100, and 200 trials of conditioning, but not after 10 trials. Although the initial magnitude of the effect was comparable among 50, 100, and 200 trials, the persistence of the effect appeared to increase with the trial number.

We also tested the dependence of the effect on the speed of conditioning motion. We found that 100 trials of conditioning at 180° s^{-1} and 360° s^{-1} caused similar increases in sequential firing, although conditioning at 60° s^{-1} was ineffective (Fig. 5b). We next asked whether the speed of the recalled spike sequence depends on the speed of conditioning motion. The speed of each recalled sequence was measured by linear regression of the RF locations of the recorded units as a function of their firing time. We found that in anesthetized rats the recall speed was similar for conditioning at 180° s^{-1} and 360° s^{-1} (~200° s^{-1}, corresponding to ~5 mm s^{-1}), which is slower than but within the same order of magnitude as the spontaneous wave speed observed with VSDI[25]. On the other hand, at the same speed of conditioning (180° s^{-1}), it was much faster in awake than in anesthetized rats (Supplementary Fig. 8a). This is likely due to the difference in the intrinsic network dynamics: While the cortical LFP showed prominent slow oscillations (0.5 – 1 Hz) under urethane anesthesia, it exhibited faster dynamics in the awake animals (Supplementary Fig. 8b). Together, these results indicate that the speed of the recalled spike sequence is determined primarily by the network dynamics rather than by the speed of conditioning motion. Thus only the sequence, but not the speed, of the learned motion is represented in the recall. In spontaneous memory reactivation in the hippocampus and prefrontal cortex, the spike sequences observed during behavior are often replayed at a compressed time scale[9, 10, 23]. Interestingly, the duration of the replayed spike sequence is also determined by the duration of the sharp wave ripple rather than reflecting the highly irregular behavior of the rat on the running track, suggesting that the sequence rather than time course of the experience is re-activated[26].

In principle, the effect we have observed in V1 could reflect circuit modifications in other brain areas (e.g., retina and thalamus). To test whether the effect requires synaptic modifications within the visual cortex, we repeated the motion conditioning experiment after local application of D(−)-2-Amino-5-phosphonopentanoic acid (D-APV), a specific NMDA receptor blocker known to block spike timing-dependent plasticity (STDP)[27, 28] in the visual cortex[29]. We found that 75 μM of APV largely blocked the conditioning-induced increase in sequential firing (Fig. 5c). However, consistent with previous studies[30], blocking NMDA receptors also led to a significant reduction in cortical firing rate (Supplementary Fig. 9), leaving open the possibility that the blockade of the conditioning effect was caused by a general reduction in cortical spiking rather than by the specific block of NMDA receptor-dependent STDP. In addition, after topical application in V1, APV may also affect the neighboring cortical area V2 (see Online Methods). Nevertheless, this result strongly suggests that the conditioning effect depends on activity-dependent modification within the visual cortex rather than in earlier stages of the visual pathway.

Dependence on brain state

Some of the awake animals in our study exhibited frequent spontaneous switching between two behavioral states: a quiet immobile state with high-amplitude, low-frequency (< 10 Hz) LFP activity, here referred to as ‘synchronized/quiet’ brain state (distinct from slow-wave sleep by its lack of UP-DOWN state oscillations), and a ‘desynchronized/active’ state with facial/whisker movement and irregular, high-frequency LFP activity[31, 32] (Fig. 6a and Supplementary Movie 1). Since cortical neuronal excitability and synaptic efficacy are

differentially influenced by neuromodulators under different brain states, we inquired whether the observed sequence recall depends on the brain state.

For 7 experiments in awake rats with frequent switching between the two brain states, we separated each recording into synchronized and desynchronized periods using cluster analysis of the LFP power spectrum (Fig. 6b; see Online Methods). The spike sequences evoked by the test cue at *S* were analyzed within each state and compared before and after conditioning. We found that for the test trials in the synchronized brain state, the pairwise cross-correlation function showed a strong increase in the slant after conditioning (Fig. 6c), and the CC distribution showed a marked rightward shift (mean CC from 0.22 to 0.37, $P = 2.4 \times 10^{-3}$, n = 7 experiments; Kolmogorov-Smirnov test; Fig. 6e). For the desynchronized state, however, conditioning did not cause an increased slant in the cross-correlation function (Fig. 6d) or a significant shift in the CC distribution (mean CC from 0.31 to 0.29, $P = 0.43$; Fig. 6f). To test whether this difference is due to different degrees of eye movement in the two brain states, we measured eye movement in each state with a video camera (see Online Methods). Although there was indeed a higher level of eye movement in the desynchronized state, the amplitude was much smaller than the RF size (s.d. < 10% of RF size; Supplementary Fig. 2) and thus unlikely to exert significant effects on the visual inputs. This indicates that although motion conditioning causes a significant change in the cortical circuit, manifestation of the change in the ensemble spiking activity depends strongly on the brain state.

DISCUSSION

Our study suggests that cue-triggered recall of a recently experienced temporal sequence, a function previously attributed to higher brain areas, could be partly supported by V1 ensemble activity. The observed increase in sequential firing may result from activity-dependent synaptic modification. The conditioning-evoked sequential spiking of neighboring neurons (Fig. 1d and Supplementary Fig. 1d) is well suited for the induction of STDP of intracortical connections, which should selectively potentiate the $S \rightarrow E$ connections and facilitate spike propagation in the same direction. This is reminiscent of Hebb's notion of sequential activation of cell assemblies in a 'phase sequence'[33]. Previous studies in V1 of anesthetized animals have demonstrated stimulus-induced RF modifications with temporal specificity comparable to STDP[34, 35]. The current study suggests that such synaptic plasticity may also modify neuronal ensemble dynamics to support sequence learning and pattern completion, consistent with theoretical predictions[36, 37].

Our study showed that a static stimulus flashed repeatedly at *S* was ineffective for enhancing sequential firing (Supplementary Fig. 4b, c), while a previous study using VSDI showed that a similar conditioning stimulus caused a significant increase in the similarity between the spontaneous and visually evoked cortical waves[25]. The difference between these findings may be attributed to multiple factors. First, while the VSDI signals reflect both supra- and subthreshold activity[38], the multielectrode recording used here measures only the spiking activity. Second, the increase in the similarity between the spontaneous and visually evoked waves observed with VSDI could be attributed at least partly to changes in the initiation sites of the spontaneous waves[25]. Whether the flashed conditioning stimulus induced any

change in the direction of wave propagation is unclear. It is possible that while the flashed conditioning can cause an increase in the excitability of the stimulated cortical region, thus the shift in the initiation sites of spontaneous waves, motion stimuli are required for enhancing the horizontal connections, leading to the increase in cue-triggered sequential firing.

The notion that the observed sequence learning is mediated by a simple synaptic mechanism without requiring high-level cognitive processes is consistent with the presence of the effect in anesthetized animals and with elimination of the effect by local APV application (Fig. 5c), although the effect of APV could be mediated by the reduction of cortical spiking rather than by the block of NMDA receptor-dependent synaptic modifications. On the other hand, the dependence of the effect on brain state (Fig. 6) points to the susceptibility of sequence recall to top-down modulations. The fact that significant effect was observed in both anesthetized and quietly awake states but not in the desynchronized active state suggests that the cue-triggered recall of a learned sequence depends on correlated activity among a large number of cortical neurons. Furthermore, the desynchronized active brain state may be associated with enhanced thalamocortical inputs and weakened intracortical connections, due to the influences of neuromodulators such as acetylcholine[39, 40]. A reduced contribution of the intracortical connections that have been modified by the motion conditioning could diminish the conditioning effect. Note that in our experiments, the rightward shift of CC distribution induced by 100 trials of conditioning was larger in the synchronized awake state (Fig. 6e) than in the anesthetized state (Fig. 3a), suggesting that learning of the sequence also depends on the brain state. In future studies with experimental control of the brain state during conditioning, it would be interesting to examine how learning depends on the brain state[41, 42], and whether recall also depends on the brain state at which the learning occurs[43].

Functionally, perception depends on both the current sensory inputs and previous experience, and their relative importance may vary across behavioral states[44]. While the desynchronized state may favor faithful representation of sensory inputs, the correlated ensemble activity in the synchronized state may carry information about previous experience. Repeated occurrence of a motion sequence in the recent past may suggest higher probability of such a sequence in the near future. The cue-triggered recall of spike sequence may thus provide a powerful mechanism for experience-dependent perceptual inference[45, 46]. From this point of view, the relatively short persistence of the effect (on the order of minutes) may be functionally advantageous, since experience from the recent past should be a good predictor only of the events in the near future. On the other hand, with more repeats of the stimulus sequence, especially if spread out over days or weeks, the effect may become more persistent. In addition to perceptual inference shortly after the experience, the cue-triggered recall we have observed may also complement the spontaneous reactivation of recent experience found in a variety of neuronal circuits[8-12, 23, 25, 47] to facilitate long-term memory consolidation.

Supplementary Material

Refer to Web version on PubMed Central for supplementary material.

ACKNOWLEDGEMENTS

We thank Drs. G. Buzsaki, H.D. Lv, H.S. Yao for comments and suggestions. This work was supported by 973 Program (2011CBA00400), SSSTC Program GJHZ0902 and the Knowledge Innovation Program of the Chinese Academy of Sciences (KSCX2-YW-R-29). Y.D. was supported in part by HHMI and M-m. P by a grant from the National Institutes of Health (NS036999).

Appendix

METHODS

Animal preparation

All experimental procedures were approved by Animal Research Advisory Committee of Shanghai Institutes for Biological Sciences, Chinese Academy of Sciences. A total of 70 adult Long-Evans rats (250 – 400 g, both male and female) were used in this study, for acute experiments under anesthesia (54 rats) and chronic recordings under an awake, head-fixed condition (16 rats). For acute experiments, the animal was anesthetized with urethane (i.p., 1.5 – 1.8 g kg^{-1}, given in two half doses with 20 – 30 min in between). Rats were restrained in a stereotaxic apparatus; body temperature was maintained at 37.5 °C via a heating pad. A 3 × 3 mm^2 craniotomy was made above the right V1 and the underlying dura was removed to allow insertion of the multielectrode array by a pneumatic insertion device (Cyberkinetics Company). The insertion depths were ~ 350-800 μm. The left eye was fixed with a metal ring to prevent eye movement and irrigated with eye drops. Following the experiment, animals were euthanized with CO_2 followed by cervical dislocation.

For chronic recording experiments, the rat was initially handled for 2 days, followed by at least 2 weeks of body-restraint training (2 – 3 hr per day), until the rat acclimated to body restraint. A surgery was then performed under ketamine (i.p., 100 mg kg^{-1}) and xylazine (i.p., 10 mg kg^{-1}) anesthesia, in which the animal was fitted with a dental cement headmount with 4 embedded mounting screws (MPX-0080-02P-C; Small Parts Inc). After 2 – 3 days of recovery, the rat was held in the head-fixing device for 1 hr per day for 3 – 5 days. Another surgery was then performed under ketamine and xylazine anesthesia to implant the multielectrode array into V1. Immediately after the surgery, gentamycin sulfate (5 mg kg^{-1}) and dexamethasone sodium phosphate (1 mg kg^{-1}) were administrated to prevent infection or inflammatory reaction. Recording began after > 30 hr of recovery. Each rat was recorded for ~1 hr per day. The experiment was stopped if the animal showed physiological signs of stress.

Recording

The electrode array was custom made with Ni-Cr alloy wire (California Fine Wire Company, CFW# 100188), consisting of 2 × 8 channels, with 250 μm between neighboring channels. Signals were recorded with the Cerebus system (Cyberkinetics Company). Spiking signals were band-pass filtered at 250 – 7500 Hz and sampled at 30 kHz; LFP was band-pass filtered at 0.3 – 250 Hz and sampled at 1 kHz. Most of the recorded spikes represent multiunit activity. In the anesthetized experiments, the threshold for spike detection was set at 3 – 4 times the noise level; in the awake experiments, the threshold was set at 4 – 5 times the noise level. The higher threshold in the awake experiments was chosen to reduce

contamination from movement artifact. Recordings were made in both superficial and deep cortical layers, and the results were combined.

For topical application of APV, a microwell was made with kwik-sil adhesive (WPI) surrounding the craniotomy. During application, 50 μl of ACSF containing 75 μM APV (Tocris) was loaded into the microwell 30 min before the experiment. We found that although APV application caused a decrease in cortical firing rate, the rate reached a steady state within 10 min after APV application (Supplementary Figure 9) and remained stable during the conditioning experiment. To estimate the size of the cortical area affected by APV, we applied the fluorescent dye FITC (Sangon Biotech, 75 μM) in the same manner as APV application and measured the spatial profile of fluorescence 30 min after application. At 2.5 mm from the center of the application area, the fluorescence dropped to < 10% of the peak value. This suggests that the effect of APV was limited to V1 and its immediate neighbor V2 (Fig. 1a), and it was unlikely to have a significant effect on other cortical areas.

Visual stimuli

Visual stimuli were programmed with Visual studio 2003 and DirectX 9 (Microsoft), generated with a PC computer containing a NVIDIA GeForce 6800 or en9800GT graphics board and presented with a XENARC 800YV VGA LCD monitor (16.3 × 12.2 cm^2, 1024 × 768 pixels, 70 Hz, maximum luminance 400 cd m^{-2}) placed 5.5 cm from the left eye, positioned such that the RFs of the recorded neurons were at the center of the monitor. For measuring RFs, we used sparse noise consisting of random flashes of bright squares (100% contrast, 9° per square, 100 ms per flash) on a black background. We then chose the points *S* and *E* at the two ends of the long axis of the RF distribution, so that most of the recorded RFs fall along the motion path. Which of the two points were chosen as *S* or *E*, however, varied randomly across experiments.

Each conditioning experiment consisted of a test period before conditioning (3.5 min), a conditioning period (0.35 – 7.6 min, depending on the number of conditioning trials, see below), and a test period after conditioning (7 min). For experiments with a conditioning speed of 180° s^{-1}, the conditioning period contained 10, 50, 100, or 200 trials of the motion stimulus. In each trial, a bright circular spot (anesthetized: 13.5°; awake: 18° in diameter, maximum luminance) moved from *S* to *E* (distance, 72 – 108°) over a period of 400 – 600 ms, repeated every 2.1 – 2.3 s. To test dependence on conditioning speed (Fig. 5b), the conditioning period contained 100 trials of motion conditioning at a speed of 60° s^{-1}, 180° s^{-1} or 360° s^{-1}, presented every 1.9 – 3.5 s (in each trial, the spot moved from *S* to *E* over a period of 200 – 1800 ms). For the control experiment shown in Figure 3e, f, the conditioning stimulus was a bar aligned to the long axis of the RF distribution of the recorded units (width, 18°, length, long axis of the RF distribution), flashed every 2.1 – 2.3 s (duration of flash, 400 – 600 ms, matching the duration of $S \rightarrow E$ motion at the speed of 180° s^{-1}). For the experiment shown in Supplementary Figure 4b, c, the conditioning stimulus was the bright spot (18° in diameter) flashed at *S* every 2.1s (duration, 100 ms). For the control experiment shown in Supplementary Figure 5, the conditioning period contained 100 trials of motion conditioning at a speed of 180° s^{-1} along a path parallel to the long axis of the RF

distribution, but shifted by 27° – 45° such that the recorded neuronal ensemble was not strongly activated by the motion stimulus.

During each test period, the same bright spot was flashed briefly (duration 100 ms) at either the starting (*S*) or the end (*E*) point of the conditioning motion trajectory at a pseudorandom sequence (presented once every 2.1 s). In a separate set of experiments (Fig. 3c), the test spot was flashed at the mid-point between *S* and *E* every 4.1 s. The test period contained 50 test trials at each location before conditioning, and 100 trials at each location after conditioning. For awake animals, only one recording experiment was performed each day. In each anesthetized animal, the interval between two consecutive experiments was > 1 hr.

Measurement of eye movements

Eye positions were recorded in two rats during both conditioning and test periods with a video camera at 30 Hz sampling rate under infra-red illumination (Supplementary Movie 1). Video files were imported into Matlab, and the pupil was semi-automatically marked by a custom-written software. Translational movement of the pupil was converted to angular rotation of the eye based on published rotation radius of the pupil, 2.26 mm[49].

Analysis

Only units with firing rates > 5 spikes s^{-1} and RF center falling between *S* and *E* of the motion trajectory were included in the analysis. After selection of the units, only experiments with ≥ 5 simultaneously recorded units were included in the study. For the data included in the final analysis, 5-16 units were recorded in each experiment. A total of 2631 units were recorded in the 206 experiments included in this study.

Spearman CC—To determine the RF location, each RF measured with sparse noise and reverse correlation was fitted with a 2-D Gaussian function (Fig. 1b and Supplementary Fig. 1b). The center of the Gaussian fit (x_i, y_i) (with the position of *S* defined as (0, 0)) was projected onto the $S \rightarrow E$ axis to determine the distance between the RF center and *S*. These RF distances were largely consistent with the spike timing of the neurons in response to the conditioning motion stimuli (Fig. 1d and Supplementary Fig. 1d). In subsequent analyses, the units were ordered according to the RF distance. For each trial of test stimulus, the spike trains of the recorded units within the window of 60 – 700 ms (anesthetized) or 40 – 500 ms (awake) after stimulus onset were analyzed. These windows were chosen to include most of the visually evoked responses while minimizing the contribution of spontaneous spikes.

Each spike train was convolved with a Gaussian filter $\frac{1}{\sqrt{2\pi\sigma^2}}e^{-t^2/2\sigma^2}$ to generate a instantaneous firing rate curve[10], and the firing time of the unit was defined as the time of the first peak of the rate curve. The main purpose of the Gaussian smoothing was to reduce the detrimental effect of outlier spikes on firing time estimation. For all 151 anesthetized experiments and 52/55 awake experiments, σ = 50 ms; for the remaining 3 awake experiments, in which LFP and spiking activity exhibited predominant ~8 Hz oscillations, we used σ = 30 ms, since the narrower Gaussian filter better matched the intrinsic dynamics of the cortical activity. The Spearman correlation coefficient (CC) between the firing time and the RF distance defined above was used to quantify sequential spiking.

Pairwise correlation—The pairwise correlation analysis was adopted from previous studies[11, 23]. Briefly, a cross-correlogram was computed between each pair of simultaneously recorded spike trains for each conditioning or test period. To reduce the contribution of spontaneous firing, only the spikes within the window of 0 – 700 ms (anesthetized) or 0 – 500 ms (awake) after stimulus onset were included. The RF distance between the cell pair was based on the projection of the center of the Gaussian fit onto the $S \rightarrow E$ axis (see above). The cross-correlograms for all pairwise combinations of the simultaneously recorded units were then divided into 9 groups based on their RF distances and averaged within each group. The difference before and after conditioning was then computed. Each averaged cross-correlogram and the difference ("*After – Before*") was then normalized to the range between 0 and 1 and plotted against the RF distance.

Brain state—To characterize the brain state, we computed the power spectrum of each 2-s segment of LFP recording and determined two power ratios, between 1 – 10 Hz and 1 – 25 Hz and between 15 – 30 Hz and 15 – 60 Hz. These frequency ranges were chosen empirically to optimize the separation between brain states. The two ratios were then used to construct a 2-D state space, with each point representing the LFP pattern in a 2-s period[50]. Fuzzy c-means cluster analysis was used to determine the boundary between the two clusters, allowing us to classify each of the 2-s recording period into either the synchronized or the desynchronized brain state. For each test period (before or after conditioning), the test trials falling into the two states were separated, and the effect of conditioning was measured by the comparison of pairwise correlation or of Spearman CC before and after conditioning within each group.

References

1. Lisman J, Redish AD. Prediction, sequences and the hippocampus. Philos Trans R Soc Lond B Biol Sci. 2009; 364:1193–1201. [PubMed: 19528000]
2. Buckner RL. The role of the hippocampus in prediction and imagination. Annu Rev Psychol. 2010; 61:27–48. [PubMed: 19958178]
3. Gelbard-Sagiv H, Mukamel R, Harel M, Malach R, Fried I. Internally generated reactivation of single neurons in human hippocampus during free recall. Science. 2008; 322:96–101. [PubMed: 18772395]
4. Lehn H, et al. A specific role of the human hippocampus in recall of temporal sequences. J Neurosci. 2009; 29:3475–3484. [PubMed: 19295153]
5. Fortin NJ, Agster KL, Eichenbaum HB. Critical role of the hippocampus in memory for sequences of events. Nat Neurosci. 2002; 5:458–462. [PubMed: 11976705]
6. Kesner RP, Gilbert PE, Barua LA. The role of the hippocampus in memory for the temporal order of a sequence of odors. Behav Neurosci. 2002; 116:286–290. [PubMed: 11996313]
7. Chiba AA, Kesner RP, Reynolds AM. Memory for spatial location as a function of temporal lag in rats - role of hippocampus and medial prefrontal cortex. Behav Neural Biol. 1994; 61:123–131. [PubMed: 8204078]
8. Wilson MA, Mcnaughton BL. Reactivation of hippocampal ensemble memories during sleep. Science. 1994; 265:676–679. [PubMed: 8036517]
9. Nadasdy Z, Hirase H, Czurko A, Csicsvari J, Buzsaki G. Replay and time compression of recurring spike sequences in the hippocampus. J Neurosci. 1999; 19:9497–9507. [PubMed: 10531452]
10. Ji D, Wilson MA. Coordinated memory replay in the visual cortex and hippocampus during sleep. Nat Neurosci. 2007; 10:100–107. [PubMed: 17173043]

11. Karlsson MP, Frank LM. Awake replay of remote experiences in the hippocampus. Nat Neurosci. 2009; 12:913–918. [PubMed: 19525943]
12. Diba K, Buzsaki G. Forward and reverse hippocampal place-cell sequences during ripples. Nat Neurosci. 2007; 10:1241–1242. [PubMed: 17828259]
13. O'Neill J, Senior TJ, Allen K, Huxter JR, Csicsvari J. Reactivation of experience-dependent cell assembly patterns in the hippocampus. Nat Neurosci. 2008; 11:209–215. [PubMed: 18193040]
14. Recanzone GH, Merzenich MM, Jenkins WM, Grajski KA, Dinse HR. Topographic reorganization of the hand representation in cortical area 3b owl monkeys trained in a frequency-discrimination task. J Neurophysiol. 1992; 67:1031–1056. [PubMed: 1597696]
15. Recanzone GH, Schreiner CE, Merzenich MM. Plasticity in the frequency representation of primary auditory cortex following discrimination training in adult owl monkeys. J Neurosci. 1993; 13:87–103. [PubMed: 8423485]
16. Fiorentini A, Berardi N. Perceptual learning specific for orientation and spatial frequency. Nature. 1980; 287:43–44. [PubMed: 7412873]
17. Karni A, Sagi D. Where practice makes perfect in texture discrimination: evidence for primary visual cortex plasticity. Proc Natl Acad Sci U S A. 1991; 88:4966–4970. [PubMed: 2052578]
18. Furmanski CS, Schluppeck D, Engel SA. Learning strengthens the response of primary visual cortex to simple patterns. Curr Biol. 2004; 14:573–578. [PubMed: 15062097]
19. Schoups A, Vogels R, Qian N, Orban G. Practising orientation identification improves orientation coding in V1 neurons. Nature. 2001; 412:549–553. [PubMed: 11484056]
20. Li W, Piech V, Gilbert CD. Perceptual learning and top-down influences in primary visual cortex. Nat Neurosci. 2004; 7:651–657. [PubMed: 15156149]
21. Niell CM, Stryker MP. Modulation of visual responses by behavioral state in mouse visual cortex. Neuron. 2010; 65:472–479. [PubMed: 20188652]
22. Bezdudnaya T, et al. Thalamic burst mode and inattention in the awake LGNd. Neuron. 2006; 49:421–432. [PubMed: 16446145]
23. Euston DR, Tatsuno M, McNaughton BL. Fast-forward playback of recent memory sequences in prefrontal cortex during sleep. Science. 2007; 318:1147–1150. [PubMed: 18006749]
24. Bringuier V, Chavane F, Glaeser L, Fregnac Y. Horizontal propagation of visual activity in the synaptic integration field of area 17 neurons. Science. 1999; 283:695–699. [PubMed: 9924031]
25. Han F, Caporale N, Dan Y. Reverberation of recent visual experience in spontaneous cortical waves. Neuron. 2008; 60:321–327. [PubMed: 18957223]
26. Davidson TJ, Kloosterman F, Wilson MA. Hippocampal replay of extended experience. Neuron. 2009; 63:497–507. [PubMed: 19709631]
27. Markram H, Lubke J, Frotscher M, Sakmann B. Regulation of synaptic efficacy by coincidence of postsynaptic APs and EPSPs. Science. 1997; 275:213–215. [PubMed: 8985014]
28. Bi G, Poo M. Synaptic modification by correlated activity: Hebb's postulate revisited. Annu Rev Neurosci. 2001; 24:139–166. [PubMed: 11283308]
29. Froemke RC, Tsay IA, Raad M, Long JD, Dan Y. Contribution of individual spikes in burst-induced long-term synaptic modification. J Neurophysiol. 2006; 95:1620–1629. [PubMed: 16319206]
30. Miller KD, Chapman B, Stryker MP. Visual responses in adult cat visual cortex depend on N-methyl-D-aspartate receptors. Proc Natl Acad Sci U S A. 1989; 86:5183–5187. [PubMed: 2567996]
31. Crochet S, Petersen CC. Correlating whisker behavior with membrane potential in barrel cortex of awake mice. Nat Neurosci. 2006; 9:608–610. [PubMed: 16617340]
32. Poulet JF, Petersen CC. Internal brain state regulates membrane potential synchrony in barrel cortex of behaving mice. Nature. 2008; 454:881–885. [PubMed: 18633351]
33. Hebb, DO. The Organization of Behavior. Wiley; New York: 1949.
34. Yao H, Dan Y. Stimulus timing-dependent plasticity in cortical processing of orientation. Neuron. 2001; 32:315–323. [PubMed: 11684000]
35. Fu YX, et al. Temporal specificity in the cortical plasticity of visual space representation. Science. 2002; 296:1999–2003. [PubMed: 12065829]

36. Abbott LF, Blum KI. Functional significance of long-term potentiation for sequence learning and prediction. Cereb Cortex. 1996; 6:406–416. [PubMed: 8670667]
37. Rao RPN, Sejnowski TJ. Predictive sequence learning in recurrent neocortical circuits. Adv Neur In. 2000; 12:164–170.
38. Grinvald A, Hildesheim R. VSDI: a new era in functional imaging of cortical dynamics. Nat Rev Neurosci. 2004; 5:874–885. [PubMed: 15496865]
39. Metherate R, Ashe JH. Nucleus basalis stimulation facilitates thalamocortical synaptic transmission in the rat auditory cortex. Synapse. 1993; 14:132–143. [PubMed: 8392756]
40. Kimura F, Fukuda M, Tsumoto T. Acetylcholine suppresses the spread of excitation in the visual cortex revealed by optical recording: possible differential effect depending on the source of input. Eur J Neurosci. 1999; 11:3597–3609. [PubMed: 10564367]
41. Ahissar E, et al. Dependence of cortical plasticity on correlated activity of single neurons and on behavioral context. Science. 1992; 257:1412–1415. [PubMed: 1529342]
42. Ego-Stengel V, Shulz DE, Haidarliu S, Sosnik R, Ahissar E. Acetylcholine-dependent induction and expression of functional plasticity in the barrel cortex of the adult rat. J Neurophysiol. 2001; 86:422–437. [PubMed: 11431522]
43. Shulz DE, Sosnik R, Ego V, Haidarliu S, Ahissar E. A neuronal analogue of state-dependent learning. Nature. 2000; 403:549–553. [PubMed: 10676963]
44. Yu AJ, Dayan P. Uncertainty, neuromodulation, and attention. Neuron. 2005; 46:681–692. [PubMed: 15944135]
45. Kersten D, Mamassian P, Yuille A. Object perception as Bayesian inference. Annu Rev Psychol. 2004; 55:271–304. [PubMed: 14744217]
46. Friston K. A theory of cortical responses. Philos Trans R Soc Lond B Biol Sci. 2005; 360:815–836. [PubMed: 15937014]
47. Ribeiro S, et al. Long-lasting novelty-induced neuronal reverberation during slow-wave sleep in multiple forebrain areas. PLoS Biol. 2004; 2:E24. [PubMed: 14737198]
48. Paxinos, G.; Watson, C. The rat brain in stereotaxic coordinates. Academic Press/Elsevier; Amsterdam, Boston: 2007.
49. Hughes A. A schematic eye for the rat. Vision Res. 1979; 19:569–588. [PubMed: 483586]
50. Gervasoni D, et al. Global forebrain dynamics predict rat behavioral states and their transitions. J Neurosci. 2004; 24:11137–11147. [PubMed: 15590930]

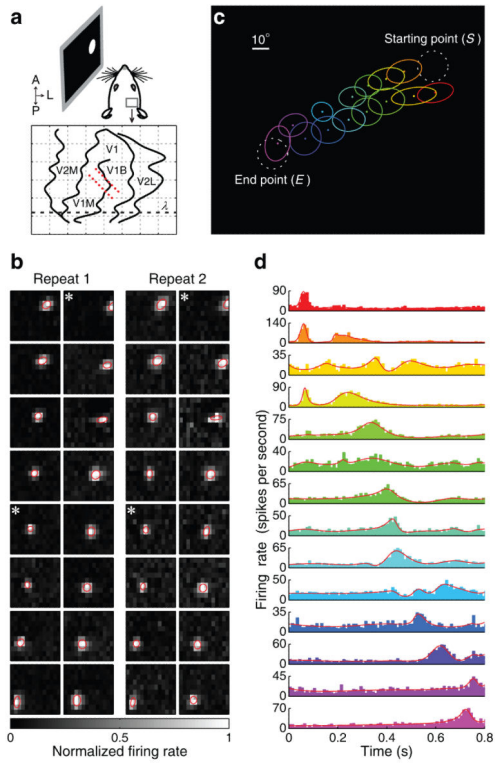

Figure 1.

Sequential spiking of neuronal ensemble in rat V1 evoked by moving spot. (**a**) Schematic of experimental setup. Visual stimuli were presented to left eye, multielectrode array (red dots) was inserted into right V1. Diagram of rat cortex was adopted from Paxinos and Watson[48], shown on 1 × 1 mm grid. A, anterior; P, posterior; L, lateral. V1, primary visual cortex. V1M, monocular region of V1; V1B, binocular region of V1; V2M, medial secondary visual cortex; V2L, lateral secondary visual cortex. λ, skull landmark lambda. (**b**) Multiunit RFs recorded simultaneously by 16 electrodes in an awake rat. Red ellipse, contour of Gaussian fit at one standard deviation. The two repeats of RF measurement were separated by 30 min. "*", units excluded from analyses because of low firing rate or extraneous RF position (see Online Methods). (**c**) Superposition of RFs and visual stimuli. Colored ellipses, Gaussian fits of RFs. White dashed circles, "Starting point" (*S*) and "End point" (*E*) of conditioning spot. (**d**) PSTHs of the 14 units shown in (**c**) during conditioning, ordered by distance between RF center and *S*. Red curves, PSTHs smoothed with Bayesian adaptive regression splines.

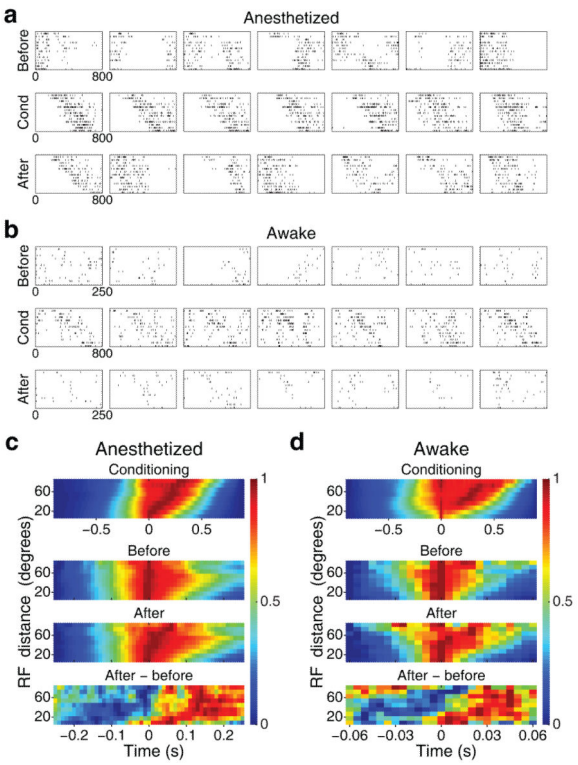

Figure 2.

Conditioning-induced increase of sequential spiking in anesthetized and awake rats. (**a**,**b**) Example spike trains of simultaneously recorded units in anesthetized (**a**, 13 units) and awake (**b**, 12 units) rats evoked by $S \rightarrow E$ conditioning ("*cond*"; middle) and by test cue at *S* before (top) and after (bottom) 100 trials of conditioning at a speed of 180° s^{-1}. Each row shows responses in 7 consecutive trials, 0 – 800 ms (**a**, middle row of **b**) or 0 – 250 ms (**b**, top and bottom rows) after stimulus onset. Units are ordered by distance between RF center and *S*. (**c**,**d**) Top three rows, pairwise cross-correlation averaged from anesthetized (**c**, n = 19 experiments) and awake (**d**, n = 18) rats with 100 trials of conditioning at 180° s^{-1}. Bottom row, difference between cross-correlation functions before and after conditioning.

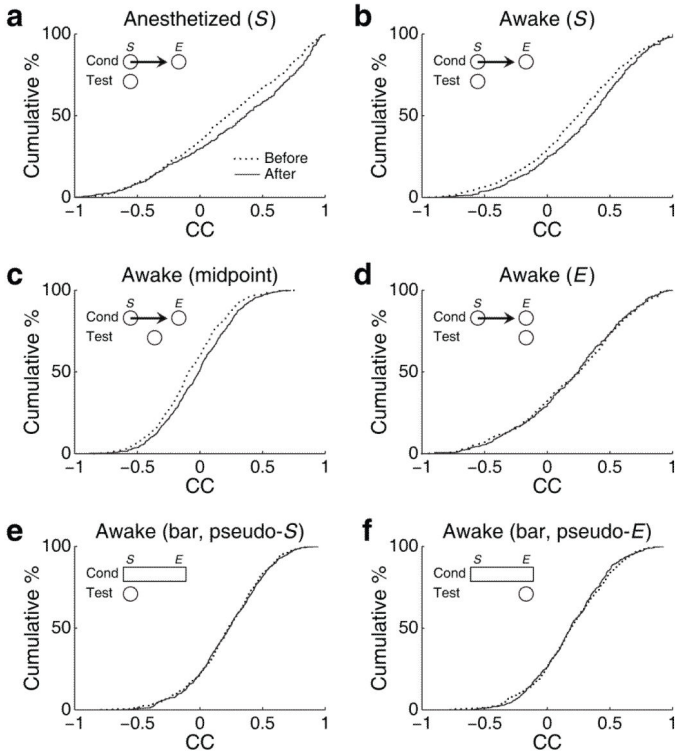

Figure 3.

Specificity of cue-triggered recall of spike sequence. (**a**,**b**) Cumulative histograms of Spearman CCs between test cue-evoked spike sequence and RF position, before (dotted line) and the first 2 min after (solid line) 100 trials of conditioning at 180° s^{-1} for anesthetized (**a**, n = 19 experiments) and awake (**b**, n = 18) rats. Note that the CC distribution before conditioning (dotted line) shows a rightward shift from CC = 0, due to symmetric spread of activity evoked by the stimulus at *S*. (**c**,**d**) Cumulative histograms of CCs for spike sequences evoked by test cues at mid-point between *S* and *E* (**c**, n = 19) and at *E* (**d**, n = 18) before (dotted line) and the first 2 min after (solid line) conditioning in awake rats. (**e**,**f**) Cumulative histograms of CCs for test stimuli at *S* (**e**) and *E* (**f**) before (dotted line) and the first 2 min after (solid line) 100 trials of flashed bar conditioning (n = 18). Since there is no directionality in the bar stimulus, the starting and end points were chosen randomly for each experiment as either of the two ends of the bar, referred to as pseudo-*S* (**e**) and pseudo-*E* (**f**), respectively. Diagram in upper left region of each plot illustrates conditioning and test stimuli used in that experiment.

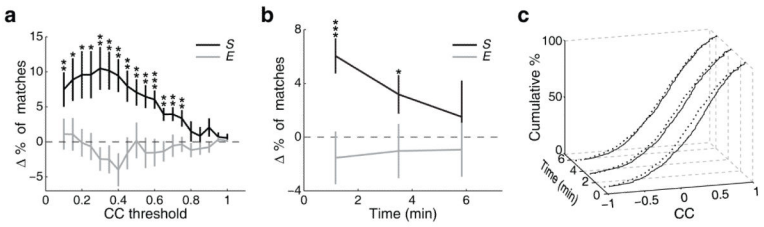

Figure 4.

Persistence of conditioning-induced increase in sequential spiking in awake rats. (**a**) Difference in percentage of sequence matches before and after conditioning vs. CC threshold for test cues at *S* (black) and *E* (gray). The difference was significant at all CC thresholds below 0.75 for *S* ("*", $P < 0.05$; "**", $P < 0.01$; "***", $P < 0.001$; Wilcoxon signed rank test), but not at any threshold for *E*. Error bar, s.e.m. (**b**) Time course for decay of conditioning-induced increase in percentage of matches (at CC threshold of 0.6). For *S*, the increase was significant at 2 min ($P = 8.6 \times 10^{-4}$; Wilcoxon signed rank test) and 4 min ($P = 0.022$), but not at 6 min ($P = 0.57$). For *E*, the effect was not significant at any time. Error bar, s.e.m. (**c**) Cumulative histograms of Spearman CCs at different periods after conditioning (solid lines). Dotted line, histogram before conditioning. The difference was significant at 2 and 4 min ($P = 1.5 \times 10^{-4}$; $P = 9.8 \times 10^{-3}$; Kolmogorov-Smirnov test), but not at 6 min ($P = 0.1$).

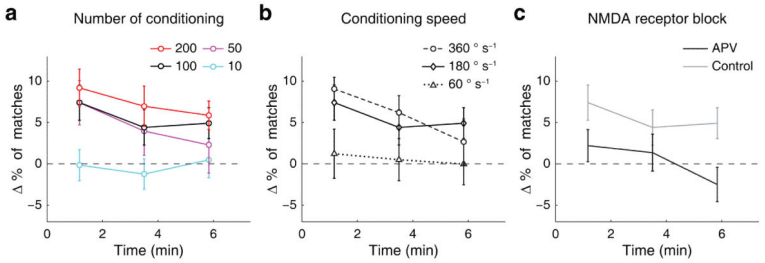

Figure 5.

Dependence of sequence learning on conditioning parameters and NMDA receptor activation, measured in anesthetized rats. (**a**) Dependence of conditioning-induced increase in sequential firing on the number of conditioning trials. Each line represents decay time course of the increase in percentage of matches (at CC threshold of 0.6) induced by a given number of conditioning trials at a speed of 180° s^{-1}. Red: 200 trials, P = 0.002, 0.01, 0.002 at 2, 4, 6 min after conditioning, n = 15; black: 100 trials, $P = 3.3 \times 10^{-3}$, 0.044, 0.027, n = 19; magenta: 50 trials, P = 0.03, 0.30, 0.42, n = 15; cyan: 10 trials, P = 0.90, 0.39, 0.87, n = 14; Wilcoxon signed rank test. (**b**) Dependence on conditioning speed. Each line represents decay time course following 100 trials of conditioning at a given conditioning speed. Dash: 360° s^{-1}, $P = 2.8 \times 10^{-4}$, 0.01, 0.23, n = 18; Solid: 180° s^{-1} (same as black line in **a**); Dotted: 60° s^{-1}, P = 0.64, 0.99, 0.41, n = 21. (**c**) Effect of local application of 75 μM APV. Black/gray line shows decay time course following 100 trials of conditioning at a speed of 180° s^{-1} with/without APV. Gray line, same as black solid line in (**a**) and (**b**). Black line, P = 0.34, 0.59, 0.18, n = 18. Error bar, s.e.m.

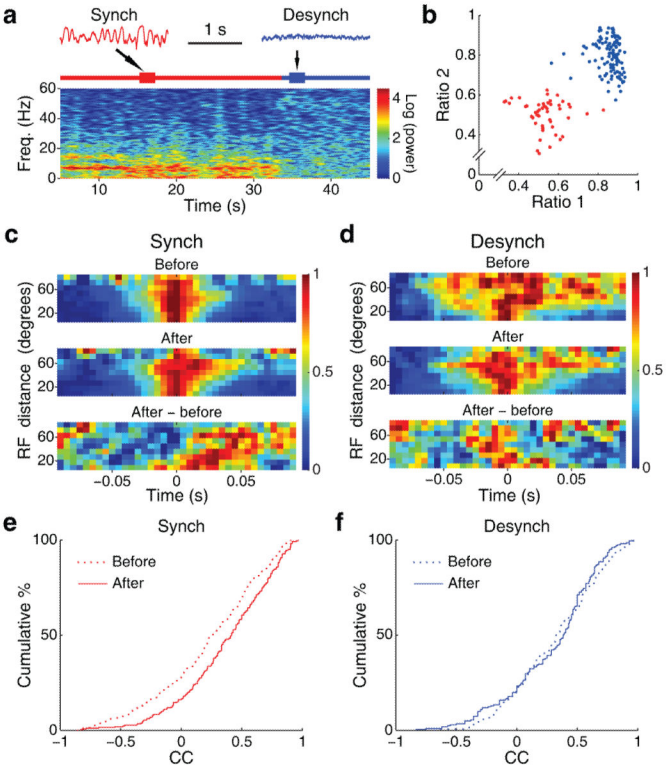

Figure 6.

Dependence of sequence recall on brain state in awake rats. (**a**) Brain state switch indicated by changes in LFP power spectrum. Red and blue lines, periods of synchronized ("*Synch*") and desynchronized ("*Desynch*") states, corresponding to red and blue clusters in (**b**). Insets above, sample LFP traces during periods marked by red and blue blocks. (**b**) Clusters in 2-D state space (Ratio 1, ratio of LFP powers between 1 – 10 Hz and 1 – 25 Hz; Ratio 2, between 15 – 30 Hz and 15 – 60 Hz). (**c**,**d**) Pairwise cross-correlations (similar to Fig. 2c, d) in synchronized (**c**) and desynchronized (**d**) states. (**e**,**f**) Cumulative histograms of Spearman CCs for test cue at *S* before (dotted line) and the first 5 min after (solid line) conditioning during synchronized (**e**) and desynchronized (**f**) states for the 7 experiments with frequent switching between the two brain states.